Computationally effective solution of the inverse problem in time-of-flight spectroscopy

Kamran, Faisal; Abildgaard, Otto Højager Attermann; Subash, Arman Ahamed; Andersen, Peter E.; Andersson-Engels, Stefan; Khoptyar, Dmitry

Published in:
Optics Express

Link to article, DOI:
10.1364/OE.23.006937

Publication date:
2015

Document Version
Publisher's PDF, also known as Version of record

Computationally effective solution of the inverse problem in time-of-flight spectroscopy

Faisal Kamran,[1,*] Otto H. A. Abildgaard,[2] Arman A. Subash,[3] Peter E. Andersen,[1] Stefan Andersson-Engels,[2] and Dmitry Khoptyar[2]

[1]*Department of Photonics Engineering, Technical University of Denmark, Denmark*
[2]*Department of Applied Mathematics and Computer Science, Technical University of Denmark, Denmark*
[3]*Department of Physics, Lund University, Sweden*
**faisal309@gmail.com*

Abstract: Photon time-of-flight (PTOF) spectroscopy enables the estimation of absorption and reduced scattering coefficients of turbid media by measuring the propagation time of short light pulses through turbid medium. The present investigation provides a comparison of the assessed absorption and reduced scattering coefficients from PTOF measurements of intralipid 20% and India ink-based optical phantoms covering a wide range of optical properties relevant for biological tissues and dairy products. Three different models are used to obtain the optical properties by fitting to measured temporal profiles: the Liemert-Kienle model (LKM), the diffusion model (DM) and a white Monte-Carlo (WMC) simulation-based algorithm. For the infinite space geometry, a very good agreement is found between the LKM and WMC, while the results obtained by the DM differ, indicating that the LKM can provide accurate estimation of the optical parameters beyond the limits of the diffusion approximation in a computational effective and accurate manner. This result increases the potential range of applications for PTOF spectroscopy within industrial and biomedical applications.

OCIS codes: (300.6500) Spectroscopy, time-resolved; (030.5620) Radiative transfer; (160.4760) Optical properties.

References and links

1. L. X. Yu, "Pharmaceutical quality by design: product and process development, understanding, and control," Pharm. Res. **25**(4), 781–791 (2008).
2. H. Huang, H. Yu, H. Xu, and Y. Ying, "Near infrared spectroscopy for on/in-line monitoring of quality in foods and beverages: A review," J. Food Eng. **87**(3), 303–313 (2008).
3. B. M. Nicolaï, K. Beullens, E. Bobelyn, A. Peirs, W. Saeys, K. I. Theron, and J. Lammertyn, "Nondestructive measurement of fruit and vegetable quality by means of NIR spectroscopy: A review," Postharvest Biol. Technol. **46**(2), 99–118 (2007).
4. M. Jamrógiewicz, "Application of the near-infrared spectroscopy in the pharmaceutical technology," J. Pharm. Biomed. Anal. **66**, 1–10 (2012).
5. Y. Roggo, P. Chalus, L. Maurer, C. Lema-Martinez, A. Edmond, and N. Jent, "A review of near infrared spectroscopy and chemometrics in pharmaceutical technologies," J. Pharm. Biomed. Anal. **44**(3), 683–700 (2007).
6. S. Tsuchikawa, "A review of recent near infrared research for wood and paper," Appl. Spectrosc. Rev. **42**(1), 43–71 (2007).
7. S. S. Tsuchikawa and M. Schwanninger, "A review of recent near infrared research for wood and paper (Part 2)," Appl. Spectrosc. Rev. **48**(7), 560–587 (2013).
8. T. Durduran, R. Choe, W. B. Baker, and A. G. Yodh, "Diffuse optics for tissue monitoring and tomography," Rep. Prog. Phys. **73**(7), 076701 (2010).
9. M. Wolf, M. Ferrari, and V. Quaresima, "Progress of near-infrared spectroscopy and topography for brain and muscle clinical applications," J. Biomed. Opt. **12**(6), 062104 (2007).
10. A. Pifferi, A. Farina, A. Torricelli, G. Quarto, R. Cubeddu, and P. Taronia, "Time-domain broadband near infrared spectroscopy of the female breast: a focused review from basic principles to future perspectives," J. Near Infrared Spectrosc. **20**(1), 223–235 (2012).

#225766 - $15.00 USD Received 27 Oct 2014; revised 19 Feb 2015; accepted 23 Feb 2015; published 6 Mar 2015

11. D. Contini, L. Zucchelli, L. Spinelli, M. Caffini, R. Re, A. Pifferi, R. Cubeddu, and A. Torricelli, "Brain and muscle near infrared spectroscopy/imaging techniques," J. Near Infrared Spectrosc. **20**(1), 15–27 (2012).
12. Q. Luo, B. Li, Z. Qiu, Z. Huang, Y. Gu, and X. D. Li, "Advanced optical techniques for monitoring dosimetric parameters in photodynamic therapy," Proc. SPIE **8553**, 85530F (2012).
13. M. S. Patterson, B. Chance, and B. C. Wilson, "Time resolved reflectance and transmittance for the non-invasive measurement of tissue optical properties," Appl. Opt. **28**(12), 2331–2336 (1989).
14. K. Shimizu, A. Ishimaru, L. Reynolds, and A. P. Bruckner, "Backscattering of a picosecond pulse from densely distributed scatterers," Appl. Opt. **18**(20), 3484–3488 (1979).
15. L. V. Wang and H. Wu, *Biomedical Optics:Pprinciples and Imaging* (John Wiley & Sons, 2012).
16. F. Martelli, S. D. Bianco, and A. Ismaelli, *Light Propagation Through Biological Tissue and Other Diffusive Media: Theory, Solution and Software* (SPIE Press, 2009).
17. E. D. Aydin, C. R. E. De-Oliveira, and A. J. H. Goddard, "A finite element-spherical harmonics radiation transport model for photon migration in turbid media," J. Quant. Spectrosc. Radiat. Transf. **84**(3), 247–260 (2004).
18. A. Liemert and A. Kienle, "Analytical solution of the radiative transfer equation for infinite-space fluence," Phys. Rev. A **83**(1), 015804 (2011).
19. A. D. Klose and E. W. Larsen, "Light transport in biological tissue based on the simplified spherical harmonics equations," J. Comput. Phys. **220**(1), 441–470 (2006).
20. M. L. Adams and E. W. Larsen, "Fast iterative methods for discrete-ordinates particle transport calculations," Prog. Nucl. Energy **40**(1), 3–159 (2002).
21. M. S. Patterson, B. Chance, and B. C. Wilson, "Time resolved reflectance and transmittance for the non-invasive measurement of tissue optical properties," Appl. Opt. **28**(12), 2331–2336 (1989).
22. E. Alerstam, W. C. Y. Lo, T. D. Han, J. Rose, S. Andersson-Engels, and L. Lilge, "Next-generation acceleration and code optimization for light transport in turbid media using GPUs," Biomed. Opt. Express **1**(2), 658–675 (2010).
23. E. Alerstam, T. Svensson, and S. Andersson-Engels, "Parallel computing with graphics processing units for high-speed Monte Carlo simulation of photon migration," J. Biomed. Opt. **13**(6), 060504 (2008).
24. A. Liemert and A. Kienle, "Infinite space Green's function of the time-dependent radiative transfer equation," Biomed. Opt. Express **3**(3), 543–551 (2012).
25. J. C. C. Day, R. Bennett, B. Smith, C. Kendall, J. Hutchings, G. M. Meaden, C. Born, S. Yu, and N. Stone, "A miniature confocal Raman probe for endoscopic use," Phys. Med. Biol. **54**(23), 7077–7087 (2009).
26. E. Alerstam, T. Svensson, S. Andersson-Engels, L. Spinelli, D. Contini, A. Dalla Mora, A. Tosi, F. Zappa, and A. Pifferi, "Single-fiber diffuse optical time-of-flight spectroscopy," Opt. Lett. **37**(14), 2877–2879 (2012).
27. A. Puszka, L. Di Sieno, A. D. Mora, A. Pifferi, D. Contini, G. Boso, A. Tosi, L. Hervé, A. Planat-Chrétien, A. Koenig, and J. M. Dinten, "Time-resolved diffuse optical tomography using fast-gated single-photon avalanche diodes," Biomed. Opt. Express **4**(8), 1351–1365 (2013).
28. E. Simon, F. Foschum, and A. Kienle, "Hybrid Green's function of the time-dependent radiative transfer equation for anisotropically scattering semi-infinite media," J. Biomed. Opt. **18**(1), 015001 (2013).
29. E. Simon, F. Foschum, and A. Kienle, "Time-resolved diffuse spectroscopy measurements using a hybrid Green's function for the radiative transfer equation," Proc. SPIE **8799**, 879906 (2013).
30. O. H. A. Nielsen, A. A. Subash, F. D. Nielsen, A. B. Dahl, J. L. Skytte, S. Andersson-Engels, and D. Khoptyar, "Spectral characterizations of dairy products using photon time-of-flight spectroscopy," J. Near Infrared Spectrosc. **21**(5), 375–383 (2013).
31. D. Khoptyar, A. A. Subash, S. Johansson, M. Saleem, A. Sparén, J. Johansson, and S. Andersson-Engels, "Broadband photon time-of-flight spectroscopy of pharmaceuticals and highly scattering plastics in the VIS and close NIR spectral ranges," Opt. Express **21**(18), 20941–20953 (2013).
32. E. Alerstam, S. Andersson-Engels, and T. Svensson, "White Monte Carlo for time-resolved photon migration," J. Biomed. Opt. **13**(4), 041304 (2008).
33. B. W. Pogue and M. S. Patterson, "Review of tissue simulating phantoms for optical spectroscopy, imaging and dosimetry," J. Biomed. Opt. **11**(4), 041102 (2006).
34. T. Svensson, E. Alerstam, D. Khoptyar, J. Johansson, S. Folestad, and S. Andersson-Engels, "Near-infrared photon time-of-flight spectroscopy of turbid materials up to 1400 nm," Rev. Sci. Instrum. **80**(6), 063105 (2009).
35. E. Alerstam, S. Andersson-Engels, and T. Svensson, "Improved accuracy in time-resolved diffuse reflectance spectroscopy," Opt. Express **16**(14), 10440–10454 (2008).
36. S. T. Flock, S. L. Jacques, B. C. Wilson, W. M. Star, and M. J. C. van Gemert, "Optical properties of Intralipid: a phantom medium for light propagation studies," Lasers Surg. Med. **12**(5), 510–519 (1992).
37. H. J. van Staveren, C. J. M. Moes, J. van Marie, S. A. Prahl, and M. J. C. van Gemert, "Light scattering in Intralipid-10% in the wavelength range of 400-1100 nm," Appl. Opt. **30**(31), 4507–4514 (1991).
38. H. Karlsson, I. Fredriksson, M. Larsson, and T. Strömberg, "Inverse Monte Carlo for estimation of scattering and absorption in liquid optical phantoms," Opt. Express **20**(11), 12233–12246 (2012).
39. E. Alerstam, *Enhancing the Performance of Time-Resolved Spectroscopy* (Lund University, 2007).
40. L. V. Wang and S. L. Jacques, "Source of error in calculation of optical diffuse reflectance from turbid media using diffusion theory," Comput. Methods Programs Biomed. **61**(3), 163–170 (2000).
41. T. Svensson, E. Alerstam, M. Einarsdóttír, K. Svanberg, and S. Andersson-Engels, "Towards accurate in vivo spectroscopy of the human prostate," J Biophotonics **1**(3), 200–203 (2008).

#225766 - $15.00 USD Received 27 Oct 2014; revised 19 Feb 2015; accepted 23 Feb 2015; published 6 Mar 2015

42. P. Di Ninni, F. Martelli, and G. Zaccanti, "The use of India ink in tissue-simulating phantoms," Opt. Express **18**(26), 26854–26865 (2010).
43. L. Spinelli, M. Botwicz, N. Zolek, M. Kacprzak, D. Milej, P. Sawosz, A. Liebert, U. Weigel, T. Durduran, F. Foschum, A. Kienle, F. Baribeau, S. Leclair, J. P. Bouchard, I. Noiseux, P. Gallant, O. Mermut, A. Farina, A. Pifferi, A. Torricelli, R. Cubeddu, H. C. Ho, M. Mazurenka, H. Wabnitz, K. Klauenberg, O. Bodnar, C. Elster, M. Bénazech-Lavoué, Y. Bérubé-Lauzière, F. Lesage, D. Khoptyar, A. A. Subash, S. Andersson-Engels, P. Di Ninni, F. Martelli, and G. Zaccanti, "Determination of reference values for optical properties of liquid phantoms based on Intralipid and India ink," Biomed. Opt. Express **5**(7), 2037–2053 (2014).
44. A. Pifferi, R. Berg, P. Taroni, and S. Andersson-Engels, "Fitting of time-resolved reflectance curves with a Monte Carlo model," in OSA Proc. Adv. Opt. Imaging Photon Migr., Proc. Top. Meet. **2**, 311–314 (1996).
45. A. Pifferi, P. Taroni, G. Valentini, and S. Andersson-Engels, "Real-time method for fitting time-resolved reflectance and transmittance measurements with a monte carlo model," Appl. Opt. **37**(13), 2774–2780 (1998).
46. S. L. Jacques, "Optical properties of biological tissues: a review," Phys. Med. Biol. **58**(11), R37–R61 (2013).
47. A. Liemert and A. Kienle, "Explicit solutions of the radiative transport equation in the P3 approximation," Med. Phys. **41**(11), 111916 (2014).

1. Introduction

Diffuse optical spectroscopy (DOS) considerably extends conventional spectroscopic analysis in turbid samples and enables monitoring of not only absorption but also scattering properties. The absorption properties of a sample is characterised by the absorption coefficient (μ_a), whereas the transport-reduced scattering coefficient (μ_s') quantifies the macroscopic scattering in a sample.

DOS thus enables practical and cost-efficient means to monitor structural properties and chemical composition of diverse samples. It is widely used for quality control [1] and process monitoring in food [2, 3], pharmaceuticals [4, 5] and timber [6, 7] industries. Other important DOS applications are in biomedical diagnostics [8–11] and medical treatment monitoring [12], respectively. For biomedical applications DOS is of particular interest due to its non- or minimally-invasive character, reducing risks for investigation-induced pain or infection.

Photon time-of-flight (PTOF) and frequency-domain techniques extend the capabilities of conventional continuous wave (CW) DOS, by separating absorption and scattering properties in comparison to merely measuring the light attenuation [13, 14]. This enriches the diagnostic potential of the technique, and provides potential for use in wider application areas.

In PTOF spectroscopy absorption and scattering are independently evaluated by monitoring of the propagation of short (picosecond) light pulses through turbid sample [15]. The evaluation generally requires solving an inverse problem where prediction from a light propagation model is fitted to the measured shape of propagated light pulses [15]. The light propagation models used for this purpose are derived from the radiative transport equation [16].

Although some options for modelling light propagation are available [17–20], until recently the practical choice was limited to either the analytical diffusion model (DM) approximation [21] or numerical Monte-Carlo simulations (MCS). Both techniques have drawbacks. The diffusion approximation assumes many scattering events, and thus its applicability range is limited to $\mu_s' \gg \mu_a$ and to large separation between the light source and detection positions in the medium. Although strongly facilitated by recent advances in parallel based GPU-computations [22, 23], MCS are still quite elaborate, time-consuming and a demanding numerical technique for solving inverse problems. In this way, the lack of universal and computationally effective analytical modelling considerably hinders wider application of DOS in many important areas including both biomedical and industrial applications.

Recently a new analytical solution to the radiative transport equation for the fluence in infinite space was presented by Liemert and Kienle [24]. On the basis of comparison to MCS, the authors claimed that their model, in the following referred as the Liemert-Kienle model (LKM), is effectively free from limitations adherent to DM, while being computationally much more efficient than MCS. If the accuracy of the model is verified in independent

#225766 - $15.00 USD Received 27 Oct 2014; revised 19 Feb 2015; accepted 23 Feb 2015; published 6 Mar 2015

studies, this result constitutes a remarkable advance in the field of DOS that strongly facilitates wider application of the technique. Indeed the claimed precision and computational simplicity of the LKM would enable high accuracy of real-time DOS measurements for the range of optical parameters, typical for biological tissue and numerous common food products. Furthermore the LKM claims to facilitate measurements at small source to detector separations, which is highly desirable for the development of miniature probes for medical and cost-efficient industrial applications [25–27].

To date the LKM has been developed and tested by the same group in comparisons to MCS only [18, 24, 28, 29]. To the best of our knowledge, the LKM has neither been evaluated by an independent group nor been used for solving the inverse problem in the infinite geometry for evaluating actual experimental data.

The objective of the present paper is thus to make the first independent evaluation of the performance of the LKM for assessing the absorption and reduced scattering coefficients of a turbid media in the infinite geometry. For this, intralipid/ink-based phantoms, measured using our photon-time-of flight spectrometer, were employed [30, 31]. We compare the LKM evaluated optical properties from such measurements to those obtained by evaluations using previously evaluated white Monte-Carlo (WMC) [32] and diffusion model (DM) [21] algorithms. In this way we also present first ever reported verification of LKM by independent comparison to MCS. The aim is to clarify the accuracy and validation range of this novel model for PTOF data analysis, and also what impact this may have for industrial and biomedical applications, respectively.

2. Materials and methods

The liquid optical phantoms were prepared from intralipid 20% (Fresenius Kabi AB, Uppsala, Sweden) and prediluted India ink (Emergo Europe, The Hague, The Netherlands) added in controlled amounts to 500 ml of tap water in a 1000 ml beaker using an Eppendorf pipette. Although the optical properties of ink and intralipid are not known with a precision better than 85% - 90% and may vary slightly from batch to batch [33], the absorption and scattering of the phantom solution is linearly proportional to the ink and intralipid concentrations, respectively. This relation is customarily used for linearity calibrations in DOS systems.

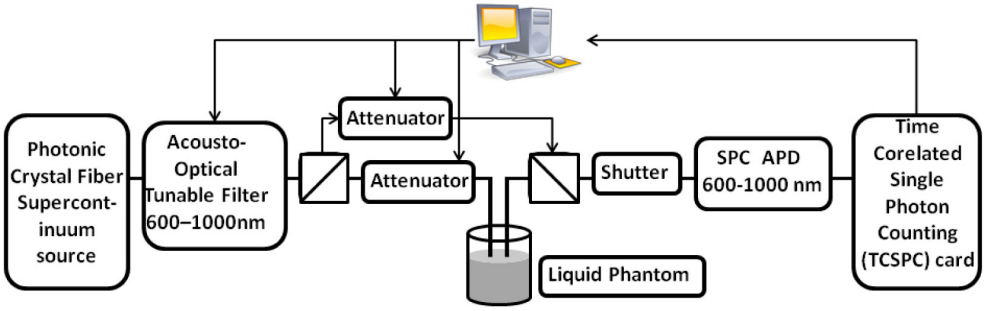

Fig. 1. Schematics of the PTOF spectrometer. SPC - Single photon counting, APD -Avalanche photodiode.

The PTOF spectrometer used for experiments was recently presented [30, 31]. The schematic of the instrument is shown in Fig. 1. To summarise, a super-continuum source (SuperK Extreme EXW 12, NKT Photonics A/S, Birkerød, Denmark) generates light pulses with a broad spectrum, from which spectrally narrow pulses are selected using a PC-controlled acousto-optical tunable filter (SuperK SELECT, NKT Photonics A/S, Birkerød, Denmark). Most of the light power is injected into the centre of the liquid phantom via a 400 μm core diameter graded index fibre. A tiny fraction of the power is routed around the sample for the purpose of timing stabilisation [31]. This timing reference further increases the

#225766 - $15.00 USD Received 27 Oct 2014; revised 19 Feb 2015; accepted 23 Feb 2015; published 6 Mar 2015

measurement accuracy by allowing for compensation of temporal drifts in the system. Both the light pulse collected at a predefined distance within the phantom and the pulse routed around it are detected by a single photon counting detector (PDM, Micro Photon Devices, Bolzano, Italy) connected to a time-correlated single photon counting (TCSPC) card (SPC-130 Becker & Hickl GmbH, Berlin, Germany). An appropriate light power for TCSPC was achieved using dedicated PC controlled optical attenuators (OZ Optics Ltd, Ottawa, Canada).

The PTOF signals were collected at a count rate of approximately 80 kHz for the duration of 32 seconds to yield approximately 2.5×10^6 counts per time-of-flight curve. The full width at half maximum of the instrument response function (IRF) is 53 ps and was taken into account during data evaluation by convolving it with the models. The IRF was measured through double-sided black printed office paper inserted between the source and detector fibres [34]. In this study we used 832 nm light. However, the actual wavelength is not of importance for model verification. The average optical power at the sample was approximately 3 mW.

The flat cut graded index fibres, inserted into thin stainless steel tubes for mechanical stability, were immersed in the phantom vertically from a metallic holder fixed to a stand. The separation between the fibres can be adjusted via a fitted micro gauge. The fibre separation was carefully measured from fibre centre to centre.

Three models for light propagation were implemented as MATLAB scripts for evaluation of μ_s' and μ_a from the recorded PTOF curves: the standard DM for isotropic media [21], a pre-calculated database based on a WMC algorithm [32, 35], and the LKM [24]. The optical properties were, in all cases, assessed with MATLAB, using a Levenberg-Marquardt algorithm on the measured PTOF data. The width of a time-bin used in the measurements was 3.0538 ps. The scattering anisotropy (g) of intralipid is not known exactly and has to be approximated. Diffuse reflectance measurements by Flock *et al*. [36] and Mie theory approximations by van Staveren *et al*. [37] suggest g = 0.79 and g = 0.62, respectively, at 832 nm. In our experiments, g = 0.7 was used for both LKM and WMC as an approximate mean value. This value was previously used for MCS [38] and has shown to produce accurate estimation for the optical properties of intralipid phantoms [32]. In all cases the thresholds for the model fitting range was set to 10% of the peak value on the rising edge and the falling edge, respectively. Additionally, a threshold of 90% of the peak value on the rising edge was also used to evaluate the optical properties with DM. The P_N-approximation RTE solution in the framework of the LKM depends on number of parameters that set balance between approximation accuracy and computational time [24]. The approximation order of N = 25 provided stabile LKM solutions in the whole range of evaluated optical properties. The other parameters, namely an approximation sphere radius of 50 mm and 100 discretization wavenumbers were used as suggested in original work by Liemert *et al*. [24]. Furthermore, in order to account for non-negligible core diameter (400 μm) of the source and detector fibres, in the analysis we average PTOF curves generated with DM and LKM over 16 distances between loci at the fibre tips, representing the distance distribution between the fibre cores [39]. WMC simulations, on the other hand, do not assume an isotropic source but are performed for a pair of fibres and their numerical aperture is already taken into account [32]. Also, WMC does not assume an isotropic source model. An example of the time resolved data set is presented in Fig. 2.

3. Results and discussion

The performance of the LKM was evaluated in two series of measurements, providing means to control its validity under conditions when the diffusion model is known to be inaccurate [35, 40]. The diffusion approximation is valid only when light has undergone a sufficiently large number of scattering events. In the first series of measurements we stepwise increased the pre-diluted ink concentration of the water/intralipid solution to gradually increase

#225766 - $15.00 USD Received 27 Oct 2014; revised 19 Feb 2015; accepted 23 Feb 2015; published 6 Mar 2015

absorption. In the second series, we tested the LKM performance by its ability to provide consistent evaluated properties at different source-detector fibre separations.

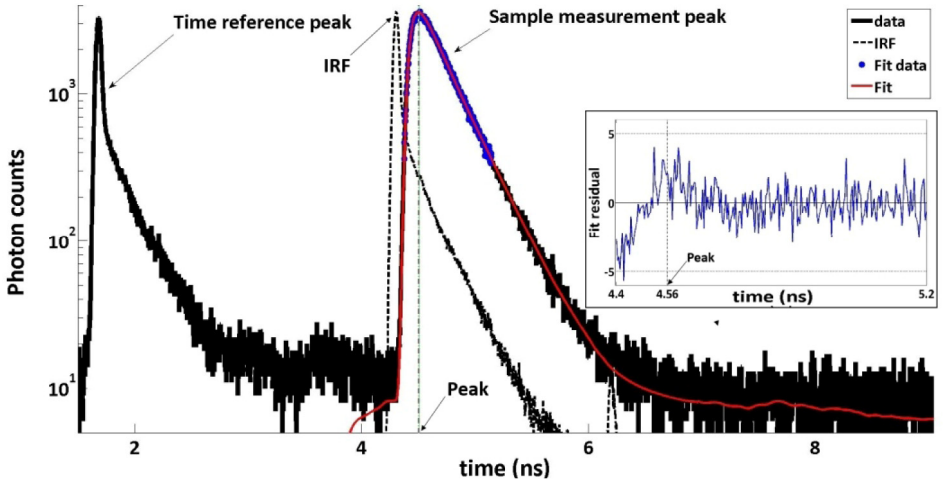

Fig. 2. An illustration of the time-resolved measurement with the tested LKM using PTOF spectroscopy and fit residuals (inset).

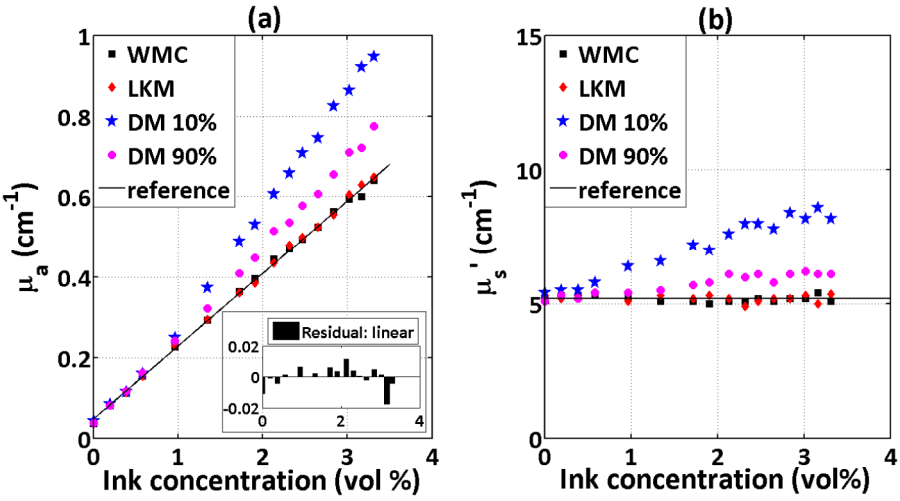

Fig. 3. Evaluated optical properties, μ_a in plot (a) and μ_s' in plot (b), presented for a ~2.8% (vol) of intralipid phantom with gradually increasing concentration of prediluted ink. Evaluations using WMC and LKM are depicted as black squares and red diamonds, respectively. The DM, with rising edge threshold at 10% of the peak and threshold at 90% of the peak, is presented with blue stars and magenta circles, respectively. The black lines present the linear fit to WMC data serving as reference value. The residual to the fit for (a) is presented in inset figure. The estimated specific absorption value for ink is 24 cm^{-1}.

In Fig. 3 the evaluated values of μ_a and μ_s' are plotted individually, for measurement series performed at 832 nm on intralipid phantoms with a reduced scattering coefficient of $\mu_s' \approx 5.2\,cm^{-1}$, and gradually increased ink concentration. The measurements were performed with a source-detector fibre separation of 15 mm, corresponding to approx. 8 times the effective scattering mean-free-path length. One can observe that the DM results in inaccurate estimations of μ_a and μ_s' when μ_a exceeds a value of approximately 0.3 cm^{-1}. In particular,

#225766 - $15.00 USD Received 27 Oct 2014; revised 19 Feb 2015; accepted 23 Feb 2015; published 6 Mar 2015

the limitation of the DM causes crosstalk in the evaluated optical parameters manifesting itself in a non-linear response in both absorption and reduced scattering with an increased ink concentration. Predictions of DM often has large errors when earlier part of the time profile before the peak is used in fitting. Therefore, we also use a threshold value of 90% of the peak on the rising edge in addition to the value of 10% to evaluate the performance of the DM. DM started to fail for higher absorption values. In contrast to DM, the values evaluated with LKM and WMC are consistent with the measurement protocol and produce a linear response in the entire evaluated absorption span. The residual of linear fit to WMC data, presented in Fig. 3(a) inset, shows the deviation of less than 4% from linear behaviour and 99% confidence interval for the slope of the regression line is 0.1807 ± 0.0051. For LKM, the deviation from linear behaviour is also less than 4%. In this study, we consider WMC as "gold standard" against which other techniques are evaluated as the accuracy of WMC with PTOFS is well established [34, 35, 41]. We note the small offset for zero ink concentration caused by residual absorption of other chromophores in the phantom. It has been shown that although the batch to batch variations of optical properties are large for India Ink, the ratio of specific absorption to extinction coefficient remains almost unchanged [42]. Using the suggested single scattering albedo value of 0.115 gives the specific extinction coefficient value of 27.1 cm^{-1}. By using the predilution ratio of $7.56x10^{-3}$ vol%, the specific absorption value of ink was estimated to be 24 cm^{-1}. This gives the absorption to extinction ratio of 0.8856. This value matches perfectly with the presented value by Ninni *et al.* [42]. Our results also fall within the range of specific absorption coefficients presented in [43] with large batch to batch deviations recorded. As it may be expected [28], LKM and WMC evaluated μ_s' remains fairly constant with measurement precision within 5% whereas μ_a grows linearly in proportion to the added ink volume. The differences between the optical parameters provided by the two techniques are within the precision of the measurements. Linearity of μ_a is observed for even very low ink concentrations [Fig. 3(a)]. This is achieved by limiting of the fitting interval at falling edge side of PTOF curve to 10% of the peak value, which removes the long photon path contribution to the fitted curve and allows avoiding influence of boundary losses. Thus, we conclude that LKM does indeed, provide as accurate values as MCS for evaluation of PTOF data in the entire range evaluated, i.e. up to $\mu_a \approx \mu_s' / 7$. Compared to WMC, LKM alleviates the need of developing new MCS and get PTOF distribution for arbitrary μ_a and μ_s'. We note that due to scalability of light propagation modelling for an isotropic infinite media [44, 45] the results of the current validation experiment can be readily generalized to other values of μ_s' corresponding to biological tissue [46], dairy products [30], and other diverse turbid samples.

Next, we investigated the dependence of the optical properties on the distance between the source and collection fibres. Ideally the evaluated μ_s' and μ_a are independent of the fibre separation. In Fig. 4, the resulting μ_s' and μ_a coefficients as evaluated by the DM, the LKM and the WMC model at various inter-fibre distances are presented for two phantoms with different optical properties. A general observation is that all models eventually break down at extremely short fibre separations, with tendency towards increased scattering and absorption. The performance of both the LKM and WMC is, however, significantly less affected at short distances in comparison to the DM. At short distance, DM model breaks down because of insufficient numbers of scattering events. In Figs. 4(c) and 4(d), we observe approximately 8.8% difference in mean absorption evaluated with WMC in high and low scattering phantoms. This difference can result from boundary effects that may have influenced our measurements specifically in the weakly scattering sample. However, it is important to note that the measured absorption values are extremely low (i.e. ca. 0.04 cm^{-1}) and by absolute value are comparable to the estimated accuracy of our setup. We also note that the apparent

#225766 - $15.00 USD Received 27 Oct 2014; revised 19 Feb 2015; accepted 23 Feb 2015; published 6 Mar 2015

breakdown of the WMC and LKM-based evaluation at the distance shorter than 6 mm does not necessarily suggest a failure of LKM, but most likely is coming from the limitations of the present experimental configuration. This may include different factors such as limitations of the finite fibre width modelling currently implemented in our evaluation script, poor temporal resolution, and inaccuracy in the estimated g value. Accurate verification of LKM performance at short inter-fibre separation would generally require higher temporal resolution of PTOF measurements than feasible with the current setup. Additionally, advanced fibre probe design may be needed in order to better fit to isotropic source approximation used in the modelling. Notably such experiment can also lead to highly accurate estimations of the intralipid scattering anisotropy (g) as it can be used as a fit parameter when using the LKM.

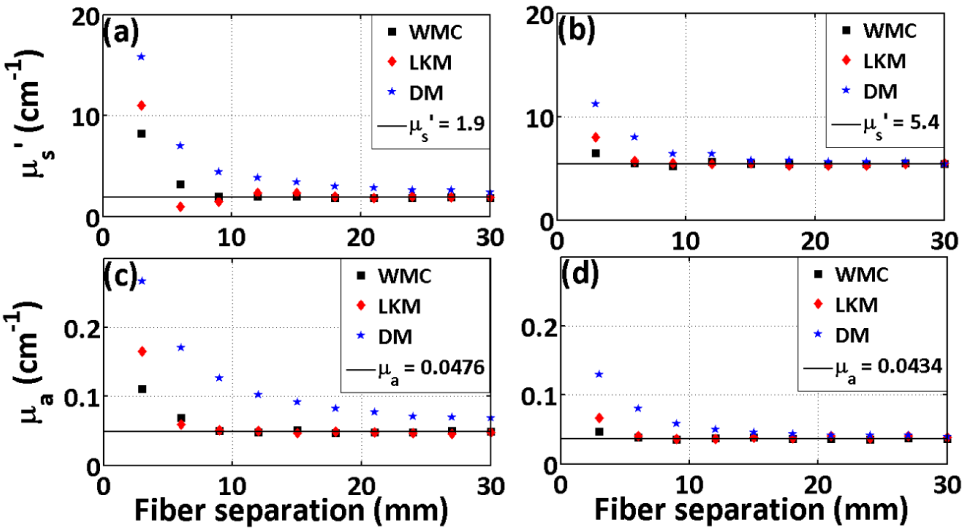

Fig. 4. Effect of source and detector fibre separation on evaluated optical properties for two different levels of scattering. The evaluated reduced scattering is presented in (a, b) and absorption in (c, d). The evaluated results by WMC, LKM and DM are depicted as black squares, red diamonds and blue stars, respectively. Black lines indicate the mean value of optical property evaluated using WMC, excluding the first 2 measurements in 'a' and 'c' and the first measurement in 'b' and 'd'.

The current findings are fully consistent with the recent LKM verification of heuristic models presented by the Kienle group [28, 29]. Eliminating the need for extensive pre computations of MC simulations, PTOF spectroscopic evaluation is computationally effective and opens a potential for future in-line applications requiring fast analysis. Additionally, the robust parameterisation presented in this article shows the strong linearity and independence of the instrument setup for the optical properties. The present assessment thus provides an independent validation of the model and robustness of the system for parameters relevant for many biomedical and industrial applications.

4. Conclusions

We presented the first independent experimental verification of a semi-analytical model for solving the radiative light transport equation in scattering turbid media in infinite geometry, recently presented by Liemert and Kienle [24]. The performance of the standard diffusion approximation, a Monte-Carlo based algorithm and the Liemert-Kienle model for evaluation of PTOF data measured on ink/intralipid solution series with various absorber concentrations and at various source-detector separations was compared. We emphasize that this is the first case that the LKM in infinite geometry is used for evaluation of experimental data and the first time it is independently verified by MCS. We observed that the LKM performs equally

#225766 - $15.00 USD Received 27 Oct 2014; revised 19 Feb 2015; accepted 23 Feb 2015; published 6 Mar 2015

well as the WMC in the range of optical and measurement parameters where diffusion approximation is inaccurate, which suggests that the LKM is a very good approximation in this parameter regime. The range of investigated optical properties covers materials ranging from biological tissue to fruits and dairy products. The availability of computationally efficient analytical approximations of the radiative transport equation constitutes an important prerequisite in the field of diffuse optical spectroscopy. The results suggest that the LKM, together with its recent extension to semi-infinite measurements geometry [47], may facilitate a broad range of applications for time-of-flight spectroscopy in the future.

#225766 - $15.00 USD Received 27 Oct 2014; revised 19 Feb 2015; accepted 23 Feb 2015; published 6 Mar 2015